Journal of Biomechanics 49 (2016) 259–266

Contents lists available at ScienceDirect

Journal of Biomechanics

journal homepage: www.elsevier.com/locate/jbiomech
www.JBiomech.com

Subject-specific multi-validation of a finite element model of ovine cervical functional spinal units

Marlène Mengoni *, Ksenija Vasiljeva, Alison C. Jones, Sami M. Tarsuslugil, Ruth K. Wilcox

Institute of Medical and Biological Engineering, School of Mechanical Engineering, University of Leeds, Leeds LS2 9JT, UK

ARTICLE INFO

Article history:
Accepted 3 December 2015

Keywords:
Functional spinal unit
Finite element
Validation
Facet joint
Intervertebral disc

ABSTRACT

The complex motion and geometry of the spine in the cervical region makes it difficult to determine how loads are distributed through adjacent vertebrae or between the zygapophysial (facet) joints and the intervertebral disc. Validated finite element modes can give insight on this distribution. The aim of this contribution was to produce direct validation of subject-specific finite element models of Functional Spinal Units (FSU's) of the cervical spine and to evaluate the importance of including fibre directionality in the mechanical description of the annulus fibrosus.

Eight specimens of cervical FSU's were prepared from five ovine spines and mechanically tested in axial compression monitoring overall load and displacements as well as local facet joints pressure and displacement. Subject-specific finite element models were produced from microCT image data reproducing the experimental setup and measuring global axial force and displacement as well as local facet joints displacement and contact forces. Material models and parameters were taken from the literature, testing isotropic and anisotropic materials for the annulus fibrosus.

The validated models showed that adding the direction of the fibres to their non-linear behaviour in the description of the annulus fibrosus improves the predictions at large strain values but not at low strain values. The load transferred through the facet joints was always accurate, irrespective of the annulus material model, while the predicted facet displacement was larger than the measured one but not significantly. This is, to the authors' knowledge, the first subject-specific direct validation study on a group of specimens, accounting for inter-subject variability.

1. Introduction

The complex motion and geometry of the spine in the cervical region makes it difficult to determine how loads are distributed through adjacent vertebrae or between the zygapophysial (facet) joints and the intervertebral disc. This distribution mechanism is an important biomechanical consideration in the investigation of surgical interventions.

Whilst finite element (FE) models allow these distributions to be investigated, they need validation for the results to be meaningful. This validation process is recognised as an important step in the development of an FE model (Viceconti et al., 2005; Jones and Wilcox, 2008), but direct, subject-specific, validations of functional spinal unit (FSU) *in-silico* models are sparse in the published literature. Jones and Wilcox (2008) reported in their review only indirect validation of spinal segment models. Since then, further indirect validation of FE models has been applied, with comparison to published data or *in-vitro* data collected on other samples, using overall range of motion or moment-rotation curves (e.g. Jebaseelan et al., 2010; Ezquerro et al., 2011; Weisse et al., 2012; Kim et al., 2013; Park et al. 2013; Mustafy et al., 2014), disc bulge or internal pressure (e.g. Moramarco et al., 2010; Kim et al., 2013, 2015), or zygapophysial contact pressure (e.g. Mustafy et al., 2014; Kim et al., 2013, 2015). The recent combination of eight validated models (Dreischarf et al., 2014) led to a better indirect validation of the pooled predictions than the individual ones when comparing overall range of motion. Whilst these studies build confidence that FE models can represent overall trends in FSU performance, they do not provide evidence of the ability to capture the varying behaviour of individual spinal units. Comparison of specimen-specific *in-silico* FSU models directly with corresponding experiments has been undertaken on only limited specimens. For example, Kalemeyn et al. (2010) and Wijayathunga et al. (2013) applied direct validation to a single FSU, comparing the moment-rotation and load-displacement behaviour respectively. Clouthier et al. (2015) assessed failure patterns on two specimens for direct validation of their fracture model. Malandrino et al. (2015) validated their disc model on one full lumbar spine under three loading types, comparing global and segmental range of motions.

* Corresponding author. Tel.: +44 113 343 5011.
E-mail address: m.mengoni@leeds.ac.uk (M. Mengoni).

http://dx.doi.org/10.1016/j.jbiomech.2015.12.005

Moreover, when validated, the level of detail required in a FSU or multi-segment *in-silico* model to reproduce *in-vitro* data is not well investigated, with only one or two subjects being included in all previously cited studies, therefore inter-subject variability was not considered. A few exceptions (Niemeyer et al., 2012; Little and Adam, 2015) generated models built from more subjects and analysed variability after indirect validation. In particular, in the last decade, FE studies started to incorporate an anisotropic model for the annulus fibrosus, considering reinforcement of a non-linear isotropic extrafibrillar matrix by non-linear highly oriented collagen fibres acting in tension only. While this type of model clearly represents the microstructure of the annulus and has a clear proven effect on the behaviour of the disc (e.g. Eberlein et al., 2001), it is not clear in what modelling situations it is actually needed.

In view of producing models to analyse the clinical effects of procedures such as vertebroplasty or disc therapies, specific attention is needed in replicating not only the overall stiffness of the modelled specimens but also the load share between intervertebral disc and facet joints or the facet joint displacement. The aims of the present work were therefore (1) to provide a direct, subject-specific, validation of ovine cervical functional spinal units FE models including global and local measurement on a population of samples; and (2) to study the necessity of inclusion of anisotropic properties for the annulus in these models.

2. Material and methods

A combined experimental and computational approach was developed to validate the *in-silico* models with local and global *in-vitro* data: apparent specimen stiffness, facet displacement, and load share between intervertebral joints (the intervertebral disc and the facet joints).

2.1. Specimen preparation and mechanical testing

The ovine spine was used in these studies due to its similarities with the human spine (Wilke et al., 1997; Alini et al., 2008), and as it is commonly used as an *in-vivo* model (Reitmaier et al., 2012; Hegewald et al., 2015).

Eight cervical FSUs were carefully excised from five mature ovine spines obtained from an abattoir. All muscle tissue and ligaments were removed from the specimens and the bone was exposed on the rear of the inferior articular facets of the superior vertebrae, taking care not to pierce the facet joint capsules. Small circular radiopaque markers were affixed to the superior side of each facet joint. The vertebrae were set in PMMA endcaps to enable flat surface testing. Another radiopaque marker was fixed to the upper PMMA surface to indicate the position of load application. The specimens were imaged using a microCT scanner (μCT100, Scanco Medical AG, Switzerland), at an isotropic voxel size of 74 μm or 89 μm depending on the size of the vertebra. Specimens were stored overnight wrapped in phosphate buffer solution soaked gauze at 5 °C. Immediately prior to testing, the ligamentous facet joint capsules were carefully cut using a scalpel to allow separation, and thin film pressure sensors (Medical Sensor 6900, Tekscan, USA) were positioned inside the joints between the cartilage surfaces (see Fig. 1). The specimens were then tested in a neutral stance simulation under axial compression, using a materials testing machine (Instron 3366, Instron, USA) at a loading rate of 1 mm/min. During testing, facet capsules were hydrated continuously with phosphate buffer solution to prevent the cartilage from drying out. The displacement was applied via a steel ball bearing, housed within a stainless steel plate (see Fig. 1). A 200 N pre-load was applied for five cycles prior the start of the measurement. Displacement-controlled compression was then applied until a load of 950 N was reached. Facet joint pressure recording was started straight after precycling. During loading, static images were taken of the facet markers at every 0.1 mm of deflection using a DSLR camera fixed onto a tripod (Canon 550d, 55–250 mm zoom lens, Japan). A ruler aligned level with the facet joints was used to scale the images. Data from the mechanical testing, pressure films, and photographs was collated for every 0.1 mm to give applied load, facet joint pressure and deflection respectively.

2.2. Finite Element modelling

Specimen-specific *in-silico* models were created with the geometry and boundary conditions based only on the experimental configuration and the microCT image data. All finite element analyses were non-linear quasi-static and run in parallel with Abaqus 6.14 (Simulia, Dassault Système).

The microCT images were scaled to a 0-255 greyscale using a bespoke script (MATLAB® R2014b, The Mathworks Inc., Natick, MA, US), and down-sampled to an isotropic 1 mm resolution. Using image processing and meshing software (ScanIP 7.1, Simpleware Ltd, Exeter, UK), the image data was segmented by direct thresholding to isolate each vertebra from the cement endcaps. As the soft tissues are not distinguishable on CT images, a procedure was developed to consistently create the cartilage layers of the facet joints and the intervertebral disc. To produce the cartilage of the upper vertebra on one of the facet joints, the lower vertebra was dilated by 2 mm and the intersection with the upper vertebra was assumed to be cartilage. Wherever this led to the two cartilage surfaces on the same joint occupying the same space, the upper cartilage was subtracted from the lower one. The intervertebral disc was produced using a morphological close operation between both vertebral bodies. A cylindrical nucleus of 11 mm diameter was created in such a way that its most posterior part aligned with the most superior part of the disc (see Fig. 2(a)).

The segmented images were meshed with linear tetrahedral elements about 1 mm in size for the bone and cement endcaps, 0.5 mm for the cartilage, and 0.8 mm for the disc tissues. The bone mesh size was based on a previous convergence study (Jones and Wilcox, 2007). A similar mesh size was used for the soft tissues since the parameters of interest were displacements rather than localised stress fields. The cement-embedded upper vertebra, lower vertebra, and the disc were exported as three meshed models into Abaqus and re-assembled assuming perfect bonding between the disc and the vertebrae. Hybrid linear element integration was used for cartilage, nucleus pulposus, and annulus fibrosus when modelled as isotropic.

Both the cement and the bone tissue were modelled with Hooke elasticity (see material parameters Table 1). In the case of bone, greyscale-specific elasticity modulus derived from previous studies was used (Wijayathunga et al., 2008; Tarsuslugil et al., 2013; Mengoni et al., 2015a). All soft-tissue material parameters were ovine-specific (Little et al., 2010; Abd Latif et al., 2012; Schmidt and Reitmaier, 2013; Reutlinger et al., 2014). Facet cartilage and nucleus materials were modelled using Neo-Hookean incompressible models. Two hyperelastic material models

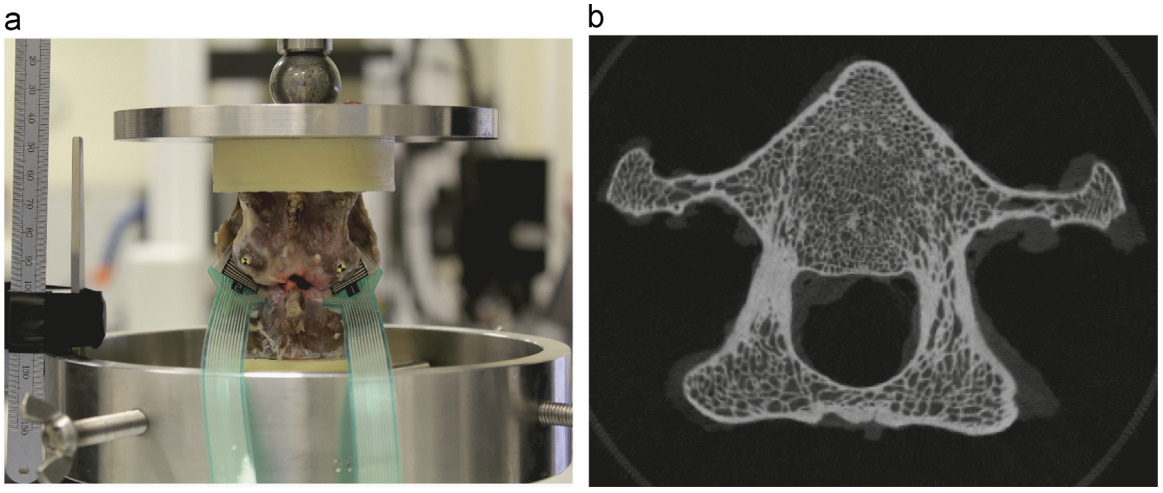

Fig. 1. (a) Experimental testing of ovine FSU with pressure reading at the facet joints, (b) axial cut of a microCT scan, showing the ovine cervical vertebra.

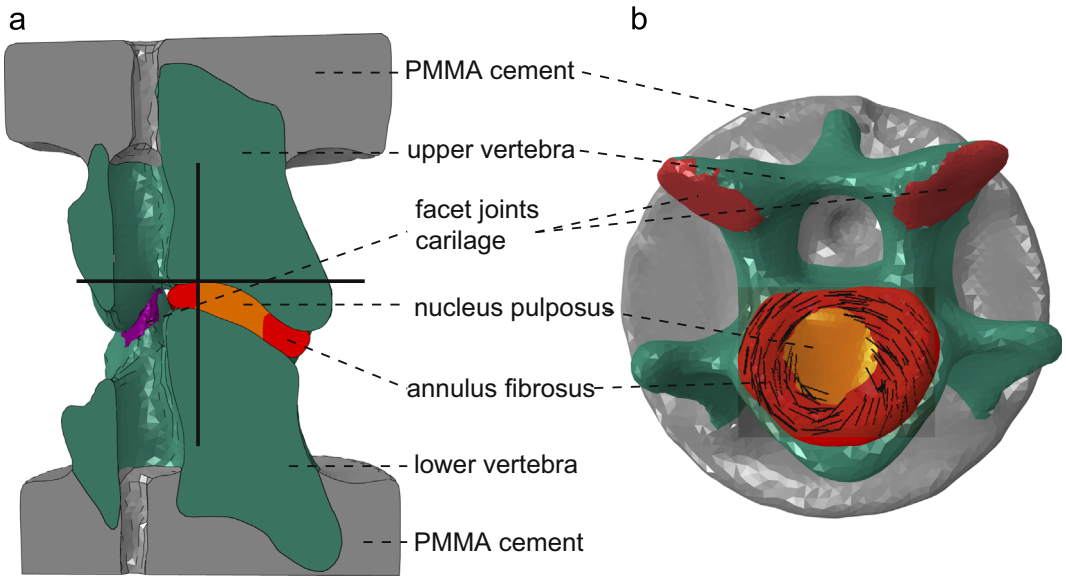

Fig. 2. (a) Sagittal cut through a reconstructed FSU from CT images; the two black lines indicate the axial and sagittal positioning of the nucleus (b) axial view of the upper vertebra and disc of the same sample; the black lines represent the local orientations of the fibres in the annulus.

were investigated for the annulus fibrosus: an anisotropic Holzapfel material (Eberlein et al., 2001; Gasser et al., 2006) and an isotropic simplified Yeoh material (Yeoh, 1993). Cartilage contact at the facet joints was modelled as a frictionless linear penalty contact.

The Holzapfel model with two homogeneous fibre directions was used (Eq. (1)). It assumes the annulus to be composed of an isotropic extrafibrillar matrix embedded with collagen fibres bearing load in tension only and distributed along two main directions:

$$W_H = \frac{1}{2}K(J-1)^2 + C_{10}(I_1-3) + \sum_a \frac{k_1}{2k_2}\left(e^{k_2(I_{4,a}-1)^2}-1\right) \quad (1)$$

where W_H is the Holzapfel strain energy density function; K, C_{10} are respectively the bulk modulus of the annulus and half the shear modulus of the annulus extrafibrillar matrix. k_1 and k_2 are collagen fibre related parameters describing their exponential stress–strain behaviour. I_1, $I_{4,a}$ and J are invariants of the Right Cauchy–Green tensor C:

$$I_1 = tr(\mathrm{C}) \quad (2)$$

$$I_{4,a} = \boldsymbol{a}^T : \mathrm{C} : \boldsymbol{a} \quad (3)$$

$$J^2 = \det(\mathbf{C}) \quad (4)$$

with $\boldsymbol{a}$ the unit vector representing the collagen fibre orientation in the reference configuration.

Material parameters k_1 and k_2 were derived from Reutlinger et al. (2014) as discussed in Mengoni et al. (2015b). C_{10} was calibrated against experimental shear data on the extrafibrillar matrix embedded with fibres (Little et al., 2010). The bulk modulus K was approximated as the bulk modulus of water, i.e. a nearly incompressible material. The collagen fibre directions were defined at $+/-$ 30° to the curved surface of the annulus, circumferentially to the axial axis of the nucleus (see Fig. 2(b)).

The Yeoh model was used to represent a fully isotropic annulus (Eq. (5)).

$$W_Y = \frac{1}{2}K(J-1)^2 + \sum_{i=1}^{3} C_{i0}(I_1-3)^i \quad (5)$$

where W_Y is the Yeoh strain energy density function; K, C_{i0} are respectively the initial bulk modulus of the annulus, and material properties describing the non-linear stress–strain behaviour. The C_{i0} material properties were calibrated against the Reutlinger et al. (2014) model of ovine lumbar annulus (see Fig. 3). The C_{10} value for the extrafibrillar matrix derived from Little et al. (2010) and used in the Holzapfel model was added to the C_{10} value obtained from that calibration.

Boundary conditions replicating the experimental tests were applied: the lower surface of the lower endcap was clamped and a rigid plane bonded to the upper surface of the upper endcap was defined to model the loading plate. A 1 mm translation in the axial direction was applied to the rigid plane centred on the load marker, while translations in the other directions were restricted and rotations were kept free to replicate the ball/plate setup and allow specimens to adjust their position freely.

The load share between intervertebral disc and facet joint, the facet joint displacement, and the load–displacement behaviour of the specimen were used to validate the modelling approach. The load share between the intervertebral disc and the facet joints was measured as the ratio of the contact load at the facet joints to the total load. The contact load at the facet joint was measured as the sum of the contact forces on the nodes of the contact surfaces of the upper vertebrae. The facet joint displacement was measured tracking the displacement in the coronal plane of the surface node closest to the central point of the facet markers. Force and facet joint displacements were compared between the *in-vitro* data and the *in-silico* data for both models using a Least-Squares linear regression and concordance correlations (R.3.1.2, R foundation for statistical computing). Given the low number of data points, load share between intervertebral disc and facet joints values were compared with an iteratively re-weighted least squares method (robust regression) and concordance correlations.

Sensitivity of the annulus material to the end-value of the applied load was assessed varying the material parameters by -20%, -10%, $+10\%$ and $+20\%$ for one of the specimens. Sensitivity to the contact model at the facet joints was assessed considering low friction contact with friction coefficients $\mu=0.05$ and $\mu=0.1$ on the same specimen.

Maximal strain values within the soft tissues at the end of loading were extracted: axial direct compressive strain of the nucleus, radial bulge of the annulus, and direct compressive strains of the cartilage at the facet joints in the direction normal to the joint surface. Values were compared between the two types of model using an independent Student's *t*-test after the normally distributed nature of the data was assessed with a Shapiro–Wilk test, using statistical software (R.3.1.2, R foundation for statistical computing).

The Python toolbox, postPro4Abq, enabling all Abaqus post-processing in this study is available from Github (Mengoni, 2015). The data associated with this paper are openly available from the University of Leeds Data Repository (Mengoni and Wilcox, 2015).

3. Results

3.1. Experimental results

The *in-vitro* load–displacement curve showed a super-linear behaviour in all cases (Fig. 4). The mean *in-vitro* load transferred from the top to the bottom vertebrae via the facets joints at the end of loading, as measured by the Tekscan pressure sensors, was 31% (st.dev. 10%) of the total load. The facet joints relative *in-vitro* displacement at the end of loading, as measured from the photographs, was generally greater than the cross-head displacement (mean 119%, st.dev. 38%), indicating some tilt of the specimens during loading (Fig. 8).

3.2. Computational results

Seven out of the eight FSU models yielded results over the full range of applied displacements. The contact slip at the facet joints

Table 1
Material parameters.

Tissue type	Elasticmodulus E (GPa)		Poisson'sratio ν (dimensionless)		Reference
Bone	Linear dependency with greyscale		0.3		Wijayathunga et al., 2008; Tarsuslugil et al., 2013; Mengoni et al., 2015a
PMMA Cement	1.035		0.3		Tarsuslugil et al., 2014
	K (MPa)	C_{10} (MPa)	k_1 (MPa)	k_2 (dimensionless)	
Annulus (anisotropic)	2200	0.03	23.92	1045.7	Little et al., 2010; Reutlinger et al., 2014
			C_{20} (MPa)	C_{30} (MPa)	
Annulus (isotropic)	2200	19.85	−91.41	24 692	Little et al., 2010; Reutlinger et al., 2014
	C_{10} (MPa)				
Cartilage	0.13				Abd Latif et al., 2012
Nucleus	0.077				Schmidt and Reitmaier, 2013

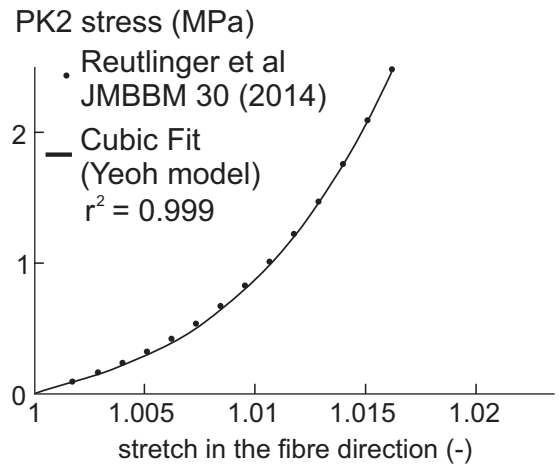

Fig. 3. Yeoh fit to the model used in Reutlinger et al. (2014).

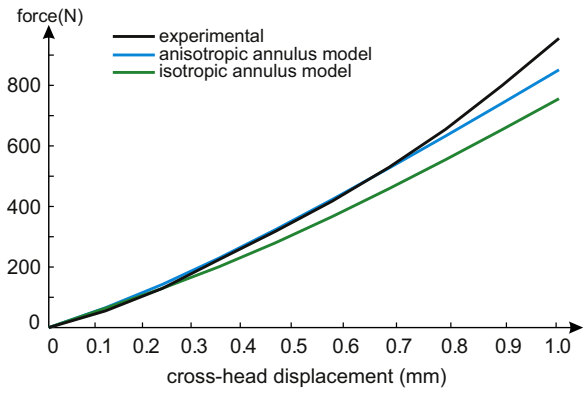

Fig. 4. Typical load/displacement curve. Black: *in-vitro* model, green: *in-silico* isotropic Yeoh model, blue: *in-silico* anisotropic Holzapfel model.

of the eighth specimen was too large and caused the vertebrae to separate from each other at an axial displacement of 0.12 mm, regardless of the annulus material model used. For the other seven models, coefficient of determination, slope of linear regression between *in-vitro* and *in-silico* values and concordance correlation coefficients assessing the deviation from the perfect prediction are presented in Table 2.

Direct comparison of *in-silico* and *in-vitro* forces, at every 0.1 mm displacement is detailed in Fig. 5. The *in-vitro* force values were predicted by the *in-silico* values with better agreement for

Table 2
Statistical comparison of *in-vitro* and *in-silico* data: CoD=coefficient of determination for the linear regression; slope=slope of the linear regression; CCC=Concordance Correlation Coefficient.

Statistical measure	Anisotropic model of the annulus			Isotropic model of the annulus		
	CoD	Slope	CCC	CoD	Slope	CCC
Force for each 0.1 mm axial displacement	0.92	0.91	0.95	0.79	1.07	0.87
Load share at the end of loading	0.79	0.88	0.70	0.88	1.02	0.93
Facet displacement at the end of loading	0.82	0.89	0.81	0.83	0.89	0.64

the anisotropic model than the isotropic model. The load transferred through the facet joints at the end of loading was predicted in the *in-silico* models at 32 ± 9% of the total load for the anisotropic model and 33 ± 5% for the isotropic one (Fig. 6). The *in-vitro* load share values were predicted by the *in-silico* values with a good agreement for both model types. Finally, the facet joints relative *in-silico* displacement at the end of loading was 123 ± 9% for the anisotropic model and 120 ± 11% for the isotropic one (Fig. 7). The *in-vitro* displacement values were predicted by the *in-silico* values with similar agreement levels for both model types.

The mean relative error in the force required for 1 mm axial displacement was 11% (st.dev. 7%) for the anisotropic model and 27% (st.dev. 6%) for the isotropic one. The maximum relative error in the force prediction over the range of applied displacement was 23% (st.dev. 12%) at the beginning of loading for the anisotropic model and 27% (st.dev. 6%) at the end of loading for the isotropic one (Fig. 8). The difference in the *in-silico* force prediction was significant ($p < 0.05$) between the two model types for displacements larger than 0.7 mm.

There was no significant difference between material models in annulus bulge values (mean 0.33 mm, st.dev. 0.12 mm) or maximum normal compressive strain in the cartilage of the facet joints (mean 38%, st.dev. 27%). Maximum axial compressive strain in the nucleus at the end of loading was significantly different between both types of model: 49% (st.dev. 12%) for the isotropic model and 35% (st.dev. 7%) for the anisotropic one ($p=0.02$).

The sensitivity results are reported in Table 3. It showed a slight decrease in the error prediction with introduction of friction for both material models but no sensitivity to the friction coefficient value. The variation in the force error due to variation in the material parameters decreased with introduction of friction in the model.

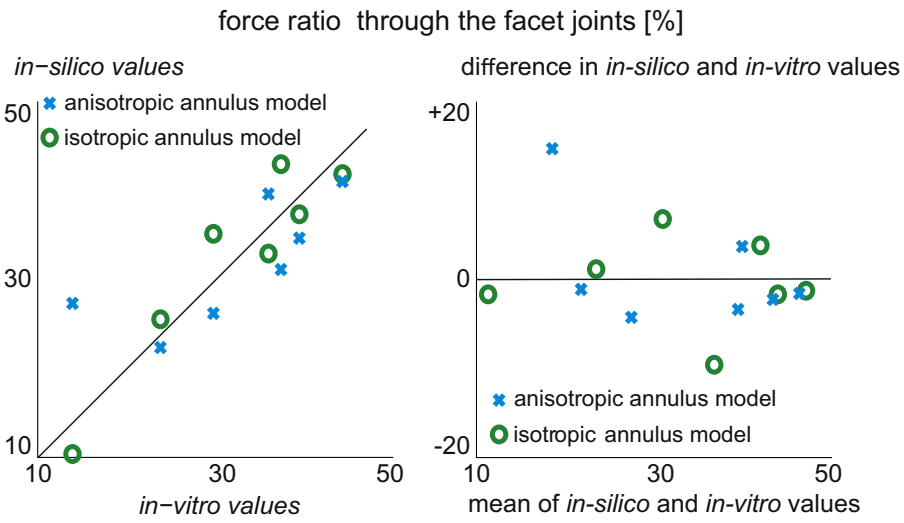

Fig. 5. Bland-Altman plot of the *in-silico* vs. *in-vitro* force function of the annulus type for each 0.1 mm axial displacement. Green circles: isotropic Yeoh model, blue crosses: anisotropic Holzapfel model (For interpretation of the references to colour in this figure legend, the reader is referred to the web version of this article.).

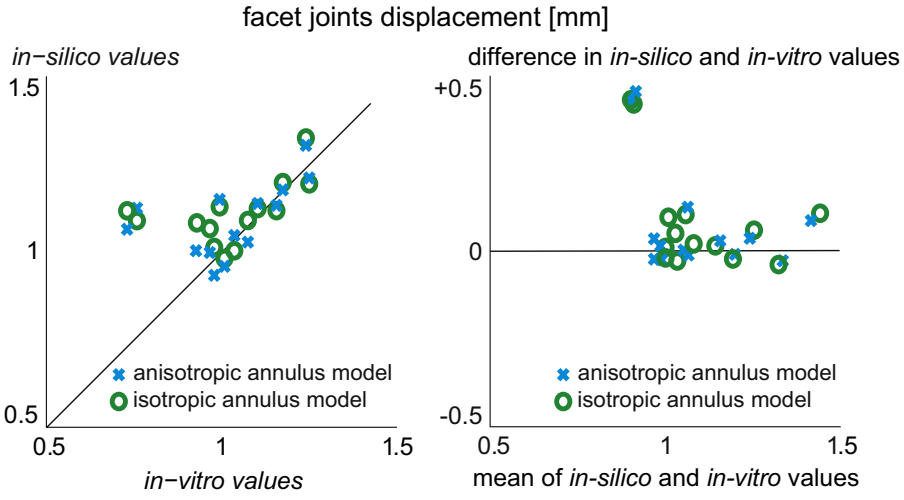

Fig. 6. Bland-Altman plot of the *in-silico* vs. *in-vitro* force ratio through the facet joints function of the annulus type at 1 mm axial displacement. Green circles: isotropic Yeoh model, blue crosses: anisotropic Holzapfel model (For interpretation of the references to colour in this figure legend, the reader is referred to the web version of this article.).

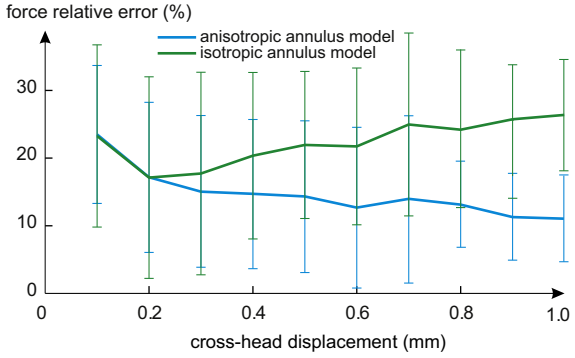

Fig. 7. Bland-Altman plot of the *in-silico* vs. *in-vitro* facet joints displacement function of the annulus type at 1 mm axial displacement. Green circles: isotropic Yeoh model, blue crosses: anisotropic Holzapfel model (For interpretation of the references to colour in this figure legend, the reader is referred to the web version of this article.).

4. Discussion

In this study, specimen-specific finite element models of FSUs were generated and compared to corresponding experimental test data. It is, to the authors' knowledge, the first subject-specific direct validation study on a group of FSU specimens. The excellent prediction of *in-vitro* data reported was achieved using specimen-specific geometry and bone tissue material parameters, where the elastic modulus was function of the grey-scale. All other material parameters were based on literature and constant across all specimens.

4.1. *in-silico prediction of in-vitro results*

The linear regression between *in-vitro* and corresponding *in-silico* data showed a good agreement and a high coefficient of determination, and the data showed a high concordance correlation coefficient, suggesting high prediction value of the *in-silico*

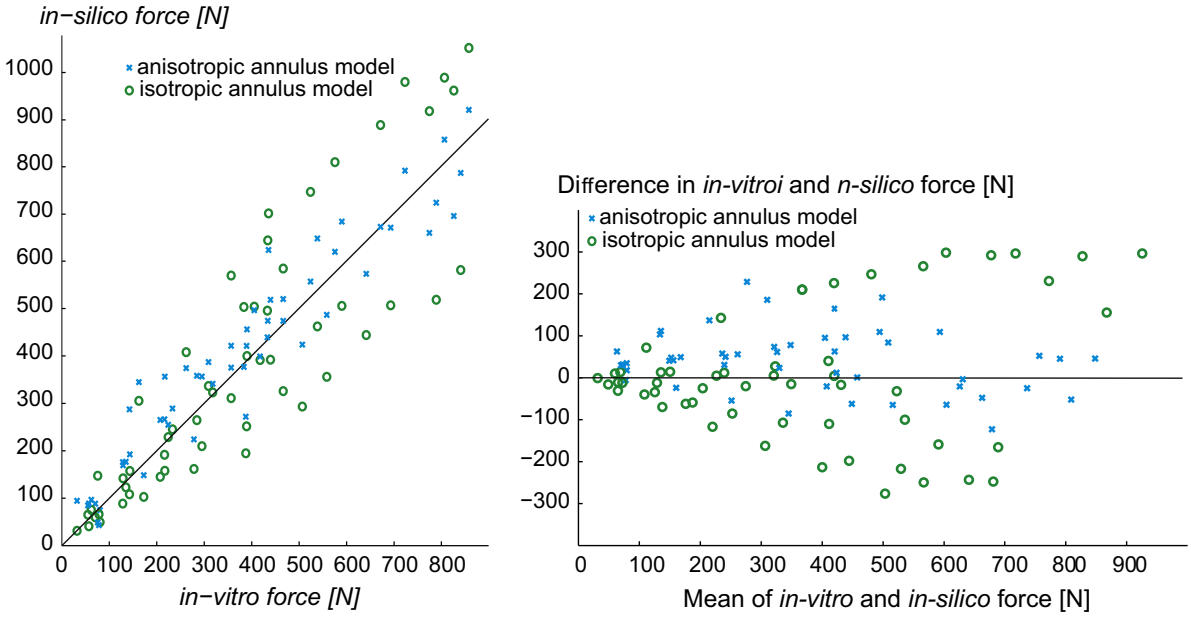

Fig. 8. Relative un-signed error in the *in-silico* force prediction (mean +/− standard deviation) function of the annulus model type. Green: isotropic Yeoh model, blue: anisotropic Holzapfel model. (For interpretation of the references to colour in this figure legend, the reader is referred to the web version of this article.)

Table 3
Difference in the force unsigned relative error at the end of the applied load compared to the baseline model; with a variation of material parameters and friction (negative sign means better relative error).

	Anisotropic model of the annulus					Isotropic model of the annulus				
Change in material parameter	−20%	−10%	+0%	+10%	+20%	−20%	−10%	+0%	+10%	+20%
No friction	+15%	+12%	Baseline	−2%	−4%	+2%	=	Baseline	+7%	+2%
Friction (μ=0.05)	+2.5%	+3%	−2%	−2.5%	−2%	+2%	+2.5%	−2.5%	−2%	−1.5%
Friction (μ=0.1)	+2.5%	+3%	−2%	−2.5%	−2%	+2%	+2.5%	−2.5%	−2%	−1.5%

approach, with a non-significant under-estimation. This indicates a direct agreement between experimental and computational data from the same specimen. Adding the direction of the fibres to their non-linear behaviour in the description of the annulus fibrosus improved the predictions of the end values of the applied force and facet displacement. The error of the predicted values for these quantities was in the order of 10% for the anisotropic model while it is about 15% for the isotropic model. The constant material properties used for the disc tissue probably explains most of the remaining error. The excellent agreement reached without specimen-specific material properties for the soft-tissues indicates that the difference in behaviour between models comes primarily from the difference in geometry. Moreover, all specimens came from young ovine tissue, reducing the tissue variability.

The difference between *in-vitro* and *in-silico* load transferred through the facet joints or facet joint displacements were always non-significant, irrespective of the annulus material model. While there was no trend in over- or under-predicting the load share, the facet joint *in-silico* displacement is slightly larger than the *in-vitro* one. This poorer agreement can be explained by the slight difference in the boundary conditions between *in-vitro* and *in-silico* setups. The *in-silico* models permitted all rotations of the plate to which the displacement was applied. In the experimental setup however, the load was applied to the plate through a ball fitting into a hole in the plate and friction occurs between the two components. This was likely to restrict the rotations of the plate in a way that was not represented in the *in-silico* models. The direct comparison of displacement and load share values showed that *in-silico* prediction were inaccurate for one specimen, with higher facet joints displacement for both models and higher load share values for the anisotropic model. Inspection of the specimen showed that the main difference of that specimen with respect to the others is a non-symmetrical facet orientation. The axial tilt of one of the joint may induce different friction behaviour on each side which is not captured I the *in-silico* model.

The results suggest that the inclusion of fibre directionality in the annulus fibrosus has an influence on the non-linearity of the model stiffness but not on the mechanism of load transfer between vertebrae. No difference is shown in the prediction of initial stiffness, maximum error in the applied force, or load share between the intervertebral disc and the facet joints. An isotropic model can therefore be used when the overall behaviour of the FSU's at relatively low loads is the output of interest. The non-significant difference in prediction accuracy of the anisotropic model does not justify its relatively complex use in that case. However and as already discussed elsewhere in the literature, the results of this study suggest that the anisotropic model is a better predictor of the non-linearity of the stiffness at higher loads, the coefficient of determination for the anisotropic model being higher than for the isotropic one. This highlights the importance of having several comparison points to validate an *in-silico* model.

The load share between the disc and the facet joints is predicted to be very similar with both types of annulus fibrosus model. This suggests that the load share is in this case mainly due to the geometry of the joints rather than the material composing those joints, in the range of relevant material models.

4.2. Limitations and challenges

Experimental measurement of the FSU during loading is challenging, particularly to capture the facet joint load transfer. Whilst the thin film transducers could measure pressure distribution over an array of points, the film rigidity could alter the size and position of the contact area, especially at the beginning of loading. Direct pressure maps comparison between experimental and computational setups was thus not considered. Only the total load transfer was used in this study. Preconditioning cycles were used to reduce bedding-in effects, but the assumed boundary conditions are still likely to be an oversimplification, particularly at low loads, which may account for the larger errors generally seen in the initial displacement steps.

Both material models for the annulus were calibrated on the same literature data, one model assumed non-linear tensile reinforcement in all directions while the other assumed that behaviour only in the fibre direction. Effectively, this leads to two different aggregate moduli for the annulus. The model validation in this work is performed for compression tests only; there is no indication of the validity of the approach and material parameters in other loading scenarios. In particular, given the reciprocal orientation of the fibres in the anisotropic model, both material models present the same stiffness in the direction of applied load. The difference in model behaviour is likely to be higher for other clinically relevant types of motions such as flexion-extension moments. The modelling procedure can however be extended to other, clinically relevant, loading types, provided a similar amount of experimental data is available for validation. Moreover, the proposed modelling approach replicates the testing conditions, i.e. quasi-static loading. In particular, the fluid content of the soft tissues, and thus the time-dependent behaviour, is not accounted for; the model is therefore not validated for cyclic loading or long term simulations.

The sensitivity study shows that the introduction of friction in the contact model at the facet joints can reduce further the force error at the end of loading. However this leads to a reduction in sensitivity in the material model and parameters. This result suggests that the introduction of friction in the model leads to the model behaviour being dictated mainly by the facet joints and not by the behaviour of the disc. While the reduced sensitivity with the introduction of friction is likely to be present in all models and outputs, it should be noted that the sensitivity study was performed on only one model and only one output was evaluated, therefore the effect on the error cannot be generalised.

The model proposed in the present work is an ovine model. While the structure of the disc and the bone is similar to that of human tissues, the anatomy is somewhat different. In particular, cervical human vertebrae are not as tall as ovine ones and the facet joint orientation is different. It is therefore likely that the inclusion of an anisotropic behaviour in the disc would have larger effects at smaller displacement values, or that models would present larger sensitivity to the cartilage friction coefficient at the facet joints.

4.3. Conclusions

The new validated procedure to prepare finite elements models from CT images of FSUs proposed here can be used to analyse other values of interest in the spine under compression. This study provided direct validation of a group of FSU models for the first time, and provided evidence on the level of detail required to reproduce an *in-vitro* axial compression protocol, accounting for inter-subject variability. The FSU models and methodologies developed can be used to assess the direct mechanical effects of interventions such as vertebroplasty or nucleus augmentation where the disc-facet load share may be compromised.

Conflicts of interest

There is no conflict of interest in this study.

Acknowledgements

This work was funded through EPSRC Grants EP/K020757/1, EP/G012172/1 and EP/F010575/1 and ERC Grant StG-2012-306615.

References

Abd Latif, M.J., Jin, Z., Wilcox, R.K., 2012. Biomechanical characterisation of ovine spinal facet joint cartilage. J. Biomech. 45 (8), 1346–1352.

Alini M., Eisenstein S.M., Ito K., Little C., Kettler A.A., Masuda K., Melrose J., Ralphs J., Stokes I., Wilke H.J. (2008) Are animal models useful for studying human disc disorders/degeneration? European Spine Journal 17(1) 2–19Brent R.P. (1971) An algorithm with guaranteed convergence for finding a zero of a function. The Computer Journal, vol. 14 (4), pp.422-425.

Clouthier, A.L., Hosseini, H.S., Maquer, G., Zysset, P.K., 2015. Finite element analysis predicts experimental failure patterns in vertebral bodies loaded via intervertebral discs up to large deformation. Med. Eng. Phys. 37 (6), 599–604.

Dreischarf, M., Zander, T., Shirazi-Adl, A., Puttlitz, C.M., Adam, C.J., Chen, C.S., Goel, V.K., Kiapour, A., Kim, Y.H., Labus, K.M., Little, J.P., Park, W.M., Wang, Y.H., Wilke, H.J., Rohlmann, A., Schmidt, H., 2014. Comparison of eight published static finite element models of the intact lumbar spine: predictive power of models improves when combined together. J. Biomech. 47 (89), 1757–1766.

Eberlein, R., Holzapfel, G.A., Schulze-Bauer, C.A.J., 2001. An anisotropic model for annulus tissue and enhanced finite element analyses of intact lumbar disc bodies. Comput. Methods Biomech. Biomed. Eng. 4 (3), 209–229.

Ezquerro, F., García Vacas, F., Postigo, S., Prado, M., Simón, A., 2011. Calibration of the finite element model of a lumbar functional spinal unit using an optimization technique based on differential evolution. Med. Eng. Phys. 33 (1), 89–95.

Gasser, T.C., Ogden, R.W., Holzapfel, G.A., 2006. Hyperelastic modelling of arterial layers with distributed collagen fibre orientations. J. R. Soc. Interface 3 (6), 15–35.

Hegewald, A.A., Medved, F., Feng, D., Tsagogiorgas, C., Beierfuß, A., Schindler, G.A., Trunk, M., Kaps, C., Mern, D.S., Thomé, C., 2015. Enhancing tissue repair in annulus fibrosus defects of the intervertebral disc: analysis of a bio-integrative annulus implant in an in-vivo ovine model. J. Tissue Eng. Regen. Med. 9 (4), 405–414.

Jebaseelan, D.D., Jebaraj, C., Yoganandan, N., Rajasekaran, S., 2010. Validation efforts and flexibilities of an eight-year-old human juvenile lumbar spine using a three-dimensional finite element model. Med. Biol. Eng. Comput. 48 (12), 1223–1231.

Jones, A.C., Wilcox, R.K., 2007. Assessment of factors influencing finite element vertebral model predictions. J. Biomech. Eng. 129 (6), 898–903.

Jones, A.C., Wilcox, R.K., 2008. Finite element analysis of the spine: towards a framework of verification, validation and sensitivity analysis. Med. Eng. Phys. 30, 1287–1304.

Kalemeyn, N., Gandhi, A., Kode, S., Shivanna, K., Smucker, J., Grosland, N., 2010. Validation of a C2–C7 cervical spine finite element model using specimen-specific flexibility data. Med. Eng. Phys. 32 (5), 482–489.

Kim, H.-J., Chun, H.-J., Lee, H.-M., Kang, K.-T., Lee, C.-K., Chang, B.-S., Yeom, J.S., 2013. The biomechanical influence of the facet joint orientation and the facet tropism in the lumbar spine. Spine J. 13 (10), 1301–1308.

Kim, H.-J., Kang, K.-T., Son, J., Lee, C.-K., Chang, B.-S., Yeom, J.S., 2015. The influence of facet joint orientation and tropism on the stress at the adjacent segment after lumbar fusion surgery: a biomechanical analysis. Spine J. 15 (8), 1841–1847.

Little, J.P., Adam, C.J., 2015. Geometric sensitivity of patient-specific finite element models of the spine to variability in user-selected anatomical landmarks. Comput. Methods Biomech. Biomed. Eng. 18 (6), 676–688.

Little, J.P., Pearcy, M.J., Tevelen, G., Evans, J.H., Pettet, G., Adam, C.J., 2010. The mechanical response of the ovine lumbar anulus fibrosus to uniaxial, biaxial and shear loads. J. Mech. Behav. Biomed. Mater. 3, 146–157.

Malandrino, A., Pozo, J.M., Castro-Mateos, I., Frangi, A.F., van Rijsbergen, M.M., Ito, K., Wilke, H.-J., Dao Tien, T., Ho Ba Tho, M.-C., Noailly, J., 2015. On the relative relevance of subject-specific geometries and degeneration-specific mechanical properties for the study of cell death in human intervertebral disc models. Front. Bioeng. Biotechnol. 3 (5), 1–15.

Mengoni, M., Sikora, S.N., d'Otreppe, V., Wilcox, R.K., Jones, A.C., 2015a. In-silico models of trabecular bone: a sensitivity analysis perspective, In: Uncertainty in Biology: A Computational Modelling Approach (part of Springer Series "Studies in Mechanobiology, Tissue Engineering and Biomaterials"). L. Geris and D. Gomez-Cabrero (Eds.). Springer International Publishing, ISBN 978-3-319-21295-1.

Mengoni, M., Luxmoore, B.J., Jones, A.C., Wijayathunga, V.N., Broom, N.D., Wilcox, R.K., 2015b. Derivation of inter-lamellar behaviour of the intervertebral disc annulus. J. Mech. Behav. Biomed. Mater. 48, 164–172.

Mengoni, M, 2015. postPro4Abq: a Python toolbox to post-process Abaqus analysis files, ⟨http://dx.doi.org/10.5281/zenodo.20601⟩.

Mengoni, M. and Wilcox, R.K., 2015. Cervical Functional Spine Units Multi-Validation Dataset. University of Leeds UK [dataset] http://dx.doi.org/10.5518/24.

Moramarco, V., Pérez del Palomar, A., Pappalettere, C., Doblaré, M., 2010. An accurate validation of a computational model of a human lumbosacral segment. J. Biomech. 43 (2), 334–342.

Mustafy, T., El-Rich, M., Mesfar, W., Moglo, K., 2014. Investigation of impact loading rate effects on the ligamentous cervical spinal load-partitioning using finite element model of functional spinal unit C2–C3. J. Biomech. 47 (12), 2891–2903.

Niemeyer, F., Wilke, H.J., Schmidt, H., 2012. Geometry strongly influences the response of numerical models of the lumbar spine – a probabilistic finite element analysis. J. Biomech. 45 (8), 1414–1423.

Park, W.M., Kim, K., Kim, Y.H., 2013. Effects of degenerated intervertebral discs on intersegmental rotations, intradiscal pressures, and facet joint forces of the whole lumbar spine. Comput. Biol. Med. 43 (9), 1234–1240.

Reitmaier, S., Shirazi-Adl, A., Bashkuev, M., Wilke, H.J., Gloria, A., Schmidt, H., 2012. In vitro and in silico investigations of disc nucleus replacement. J. R. Soc. Interface 9 (73), 1869–1879.

Reutlinger, C., Bürki, A., Brandejsky, V., Ebert, L., Büchler, P., 2014. Specimen specific parameter identification of ovine lumbar intervertebral discs: on the influence of fibre-matrix and fibre-fibre shear interactions. J. Mech. Behav. Biomed. Mater. 30, 279–289.

Schmidt, H., Reitmaier, S., 2013. Is the ovine intervertebral disc a small human one? A finite element model study. J. Mech. Behav. Biomed. Mater. 17, 229–241.

Tarsuslugil, S.M., O'Hara, R.M., Dunne, N.J., Buchanan, F.J., Orr, J.F., Barton, D.C., Wilcox, R.K., 2013. Development of calcium phosphate cement for the augmentation of traumatically fractured porcine specimens using vertebroplasty. J. Biomech. 46 (4), 711–715.

Tarsuslugil, S.M., O'Hara, R.M., Dunne, N.J., Buchanan, F.J., Orr, J.F., Barton, D.C., Wilcox, R.K., 2014. Experimental and computational approach investigating burst fracture augmentation using PMMA and calcium phosphate cements. Ann. Biomed. Eng. 42 (4), 751–762.

Yeoh, O.H., 1993. Some forms of the strain energy function for rubber. Rubber Chem. Technol. 66 (5), 754–771.

Viceconti, M., Olsen, S., Nolte, L.P., Burton, K., 2005. Extracting clinically relevant data from finite element simulations. Clin. Biomech. 20 (5), 451–454.

Wijayathunga, V.N., Jones, A.C., Oakland, R.J., Furtado, N.R., Hall, R.M., Wilcox, R.K., 2008. Development of specimen-specific finite element models of human vertebrae for the analysis of vertebroplasty. Proc. Inst. Mech. Eng. Part H. – J. Eng. Med. 222 (2), 221–228.

Wijayathunga, V.N., Oakland, R.J., Jones, A.C., Hall, R.M., Wilcox, R.K., 2013. Vertebroplasty: patient and treatment variations studied through parametric computational models. Clin. Biomech. 28 (8), 860–865.

Wilke, H.J., Kettler, A., Claes, L.E., 1997. Are sheep spines a valid biomechanical model for human spines? Spine 22, 2365–2374.

Weisse, B., Aiyangar, A.K., Affolter, Ch, Gander, R., Terrasi, G.P., Ploeg, H., 2012. Determination of the translational and rotational stiffnesses of an L4–L5 functional spinal unit using a specimen-specific finite element model. J. Mech. Behav. Biomed. Mater. 13, 45–61.